2950 Niles Road, St. Joseph, MI 49085-9659, USA
269.429.0300 fax 269.429.3852 hq@asabe.org www.asabe.org

An ASABE Meeting Presentation

Paper Number: 083637

Estimating Seasonal ET from Multispectral Airborne Imagery: An Evaluation of Interpolation-Extrapolation Techniques

José L. Chávez, Ph.D., Agricultural Engineer

USDA-ARS Conservation and Production Research Laboratory, P.O. Drawer 10, Bushland, Texas, 79012, jose.chavez@ars.usda.gov

Prasanna H. Gowda, Ph.D., Agricultural Engineer

USDA-ARS Conservation and Production Research Laboratory, P.O. Drawer 10, Bushland, Texas, 79012, prasanna.gowda@ars.usda.gov

Terry A. Howell, Ph.D., Research Leader, Agricultural Engineer

USDA-ARS Conservation and Production Research Laboratory, P.O. Drawer 10, Bushland, Texas, 79012, terry.howell@ars.usda.gov

Christopher M.U. Neale, Ph.D., Professor, Agricultural Engineer

Utah State University, 4105 Old Main Hill, Logan, Utah, 84322, cneale@cc.usu.edu

Karen Copeland, M.Sc., Soil Scientist

USDA-ARS Conservation and Production Research Laboratory, P.O. Drawer 10, Bushland, Texas, 79012, karen.copeland@ars.usda.gov

Written for presentation at the
2008 ASABE Annual International Meeting
Sponsored by ASABE
Rhode Island Convention Center
Providence, Rhode Island
June 29 – July 2, 2008

Abstract. *Irrigated agriculture in the Texas High Plains uses over 90% of the ground water from the Ogallala Aquifer. Efficient water use through improved irrigation scheduling is expected to moderate the aquifer decline rate and improve sustainability. Thus, an accurate estimation of spatial actual* *daily and seasonal evapotranspiration (ET) is needed. Remote sensing may be used for monitoring distributed actual ET. Therefore, during 2007, the Bushland Evapotranspiration and Agricultural Remote Sensing Experiment (BEAREX07) was conducted at the USDA-ARS Conservation and Production Research Laboratory (CPRL), Bushland, Texas. During BEAREX07, high resolution aircraft imagery (0.5 m pixel size in the visible and near-infrared bands and 1.8 m in the thermal band) were acquired during the cropping season using the Utah State University airborne multispectral digital system. Actual instantaneous ET was estimated using a two-source energy balance algorithm and extrapolation to daily values was performed using the evaporative fraction and the grass reference ET fraction (ET_oF). Cumulative/seasonal ET was estimated using ET_oF and cumulative grass reference ET. Data from four weighing lysimeters, in sorghum and corn fields, were used for evaluating ET predictions. Instantaneous ET was predicted with mean bias error (MBE) and root mean square error (RMSE) of 0.05 and 0.1 mm h^{-1} respectively. Daily ET was better extrapolated by the ET_oF method (error of 0.6±0.8 mm d^{-1}, MBE±RMSE); while seasonal ET was slightly under-predicted for the short period of June and July by 8.9±30.4 mm. It appears that the aerodynamic resistance, in the soil sensible heat flux, has to be neglected under low biomass [leaf area index (LAI) ≈ 0.5 m^2 m^{-2}] and heterogeneous vegetation cover conditions. Furthermore, at LAI values around 5.0 m^2 m^{-2}, ET was over-predicted perhaps due to errors in estimating the fraction of LAI that is green, the clumping factor, the vegetation fraction, soil heat flux, and/or the soil resistance to heat flux term.*

Keywords. Evaporation fraction, grass reference evaporation fraction, latent heat flux, advection.

Introduction

Remote sensing (RS) of surface energy balance (EB, Equation 1) for land provides instantaneous estimates of latent heat flux (LE) or evapotranspiration (ET_i). Instantaneous ET predictions need to be extrapolated to daily (24 h) ET rates (ET_d) to be used in the monitoring of spatially distributed crop water use, to schedule irrigations, and in general hydrologic models. Moreover, seasonal ET may be used to assess the overall irrigation project efficiency, provided volumes of water pumped (or diversions) had been measured.

$$R_n = G + H + LE \tag{1}$$

where, R_n is net radiation, G is the soil heat flux, and H is sensible heat flux. Units in Eq. 1 are all in W m^{-2} with R_n positive toward the crop surface and other terms positive away from the surface.

Brutsaert and Sugita (1992) assumed that the partitioning of available energy (AE = R_n – G), into H and LE was constant (self-preservation of AE partitioning) or that the evaporative fraction (EF = LE/AE) remains almost constant during daytime. Zhang and Lemeur (1995) added that the EF indicates how much of the AE is used for ET and that the assumption that instantaneous EF was representative of the daily energy partitioning was an acceptable approximation for extrapolating ET under clear-sky conditions.

Another method proposed by Trezza (2002) is the alfalfa reference evapotranspiration fraction (ET_rF); which uses the ratio of ET_i (hourly or shorter period) to alfalfa reference ET (ET_r). Trezza (2002) indicted that ET_rF was a better indicator of AE under advective conditions. However, according to Colaizzi et al. (2006), a better factor to scale ET_i to daily values would be ET_oF (grass reference ET fraction) instead of ET_rF, for the conditions that are common in the Texas High Plains (THP).

In terms of remote sensing energy balance models, there are several algorithms available in the literature (Gowda et al., 2008 and Gowda et al., 2007). Most of the EB models are single source models, e.g. SEBI (Menenti and Choudhury, 1993), SEBAL (Bastiaanssen et al., 1998), SEBS (Su , 2002), METRIC (Allen et al., 2007), etc. These models estimate the different components of the EB assuming the surface heat fluxes originate from a source that is the composite of vegetation and background soil.

On the other hand, algorithms as the two source energy balance model (TSM) proposed by Norman et al. (1995) are more physically based and differentiate or partition the EB terms, R_n, H and LE between the soil and the vegetation canopy. As used by Norman et al. (1995), G is a function of the soil net radiation only ($G = 0.35 \times R_{n\_soil}$); where R_{n_soil} (W m^{-2}) is the net radiation budget at the soil surface (soil only).

Since the TSM is more physically based, and allegedly it is able to discriminate heat fluxes generated from vegetated and bare soils, then it is expected to yield more accurate distributed ET_i values.

Therefore, the main objectives of this study were to a) assess the performance of a TSM in deriving ET_i values using airborne remote sensing imagery and weather station data, b) assess the capability of the EF and ET_oF methods to extrapolate ET_i to daily values, and c) test the applicability of a method in estimating seasonal ET under the advective conditions of the THP.

Material and Methods

Study Area

This study was conducted at the USDA-ARS, Conservation and Production Research Laboratory (CPRL), located in Bushland, Texas. The geographic coordinates of the CPRL are 35º 11’ N, 102º 06’ W, and its elevation is 1,170 m above mean sea level. Soils around Bushland are classified as slowly permeable Pullman clay loam soils. The major crops in the region are corn, sorghum, winter wheat, and cotton.

Remote Sensing System

The remote sensing system used in this study was the Utah State University (USU) airborne digital multispectral system. The USU system consisted of high resolution imagery in the visible, near-infrared, and thermal-infrared portions of the electromagnetic spectrum. We used three airborne remote sensing scenes acquired over the USDA-ARS, CPRL, on June 25 (DOY 176), July 10 (DOY 191), and July 26 (DOY 207) respectively. All three overpasses occurred close to 11:30 a.m. CST. These images were calibrated and transformed into surface reflectance and temperature images used for the estimation of reflected outgoing shortwave and longwave radiation, respectively, with both components required in the estimation of spatially distributed net radiation. Detailed procedure for the estimation of net radiation, using remote sensing inputs, can be found in Chávez et al. (2005). Soil heat flux was estimated as indicated in Norman et al. (1995).

The USU multispectral system comprises three Kodak[1] Megaplus digital frame cameras with interference filters centered in the green (Gn) (0.545-0.560 μm), red (R) (0.665-0.680 μm), and near-infrared (NIR) (0.795-0.809 μm) portions of the electromagnetic spectrum. The fourth camera is an Inframetrics 760 thermal-infrared scanner (8-12 μm) that provides thermal-infrared radiance, used to obtain surface radiometric temperature images.

Figure 1 shows false color composite images (NIR, R, and Gn bands) of the study site for (a) DOY 176, (b) DOY 191, and (c) DOY 207.

The USU system flew at an altitude of approximately 1,000 m (above ground level), which resulted in a 0.5 m pixel resolution for the visible and near-infrared bands and 1.8 m for the thermal band.

Radiometric and Atmospheric Calibration of Aircraft Data

The shortwave images were corrected for lens vignetting effects and geometric distortions in procedures similar to those described by Neale and Crowther (1994) and Sundararaman and Neale (1997). The individual spectral images were registered into three band images and rectified to a digital orthophotoquad base map.

The digital numbers of the rectified multispectral image were converted to radiance using the system calibration method described by Neale and Crowther (1994). These radiances were divided by the incoming solar irradiance to obtain surface spectral reflectance. Solar irradiance in each spectral band was obtained form radiance measurements made concurrently to the flights with an Exotech radiometer placed over a barium sulfate standard reflectance panel with known bidirectional properties (Jackson et al., 1992).

---

[1] The mention of trade names of commercial products in this article is solely for the purpose of providing specific information and does not imply recommendation or endorsement by the U.S. Department of Agriculture.

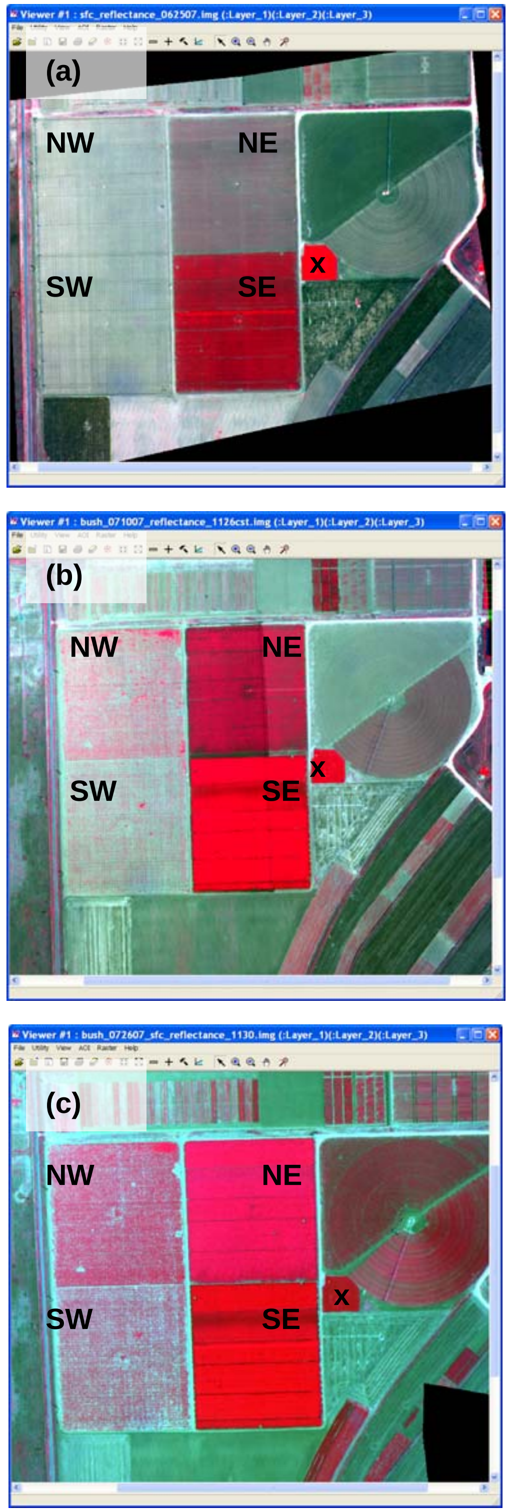

Figure 1. False color reflectance images for (a) DOY 176, (b) DOY 191, and (c) DOY 207 showing the lysimeters fields NW, NE, SE, and SW plus the weather station location (x).

The thermal infrared imagery was rectified to the high-resolution three-band images described above. The digital numbers were transformed into apparent (at sensor or brightness) temperature values using the Inframetrics 760 thermal scanner system calibration bar at the bottom of each image. The surface brightness temperature images were corrected for atmospheric effects considering surface thermal emissivity and using the atmospheric radiative transfer model MODTRAN4 v3 (Berk et al., 2003). These corrections resulted in at-surface radiometric temperatures (T_{sfc}).

Two Source Model-based Remote Sensing ET

The TSM proposed by Norman et al. (1995) and Kustas and Norman (2000) were used to apply the EB algorithm to derive ET_i from the aircraft imagery and weather station data. This EB model, as input, needs radiometric surface temperature (T_{sfc}, K), air temperature (T_a, K), horizontal wind speed (U, m s^{-1}), leaf area index (LAI, m^2 m^{-2}), vegetation fraction cover (F_c), fraction of LAI that is green (f_g), crop height (h_c, m), average leaf width (w, m), and net radiation.

Basically, the TSM algorithm solves Eq. 1 for LE after finding separately the canopy R_n and H and the soil R_n, G and H components, i.e. the TSM partitions each of the surface energy balance components into fluxes generated from the vegetation canopy (first source) and the bare soil/background soil (second source) as depicted in Fig. 2. For instance, H was estimated by adding the soil sensible heat flux (H_s) that occurs between the soil surface and a point above the canopy (Z_h), where air temperature (T_a) is measured, with the canopy sensible heat flux (H_c) generated between the vegetation canopy and a parcel of air at Z_h, assuming a parallel resistance network (Fig. 2).

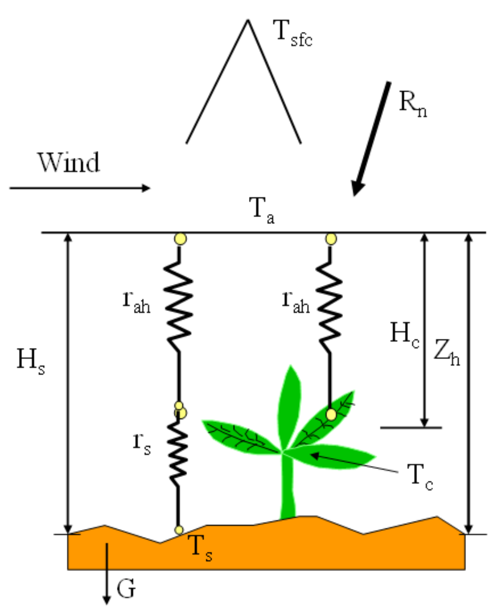

Figure 2. TSM parallel resistance network scheme.

Mathematically H is expressed as:

$$H = H_c + H_s \quad (2)$$

$$H_c = \rho_a\ Cp_a\ (T_c - T_a) / r_{ah} \quad (3)$$

$$H_s = \rho_a\ Cp_a\ (T_s - T_a) / (r_{ah}\ r_s) \quad (4)$$

$$r_s = 1 / (0.004 + (0.012 \times U_s)) \quad (5)$$

where, T_c is canopy temperature (K), T_s is soil temperature (K), r_s is the resistance to heat flow above the soil (s m^{-1}), r_{ah} is aerodynamic resistance (s m^{-1}) to heat transfer, U_s is horizontal wind speed (m s^{-1}) just above the soil surface, ρ_a is air density (kg m^{-3}), and Cp_a is specific heat of dry air (1,004 J kg^{-1} K^{-1}).

T_c and T_s were estimated using Eq. 6 for a Nadir looking thermal infrared remote sensor as:

$$T_{sfc} = [f_c\ (T_c)^4 + (1 - f_c)\ (T_s)^4]^{1/4} \quad (6)$$

where, T_{sfc} is the so-called "ensemble (or composite) surface radiometric temperature," and f_c is the fractional vegetation cover (function of LAI). First, to obtain H, an initial estimation of H_c, applying Priestly and Taylor (1972) model, is performed. Subsequently, the H_c value is used to derive an initial T_c value by inverting Eq. 3 assuming a neutral atmospheric stability condition. Next, Eq. 6 is solved for T_s and updated values of H_c and H_s are computed correcting r_{ah} for atmospheric stability using the Monin-Obukhov atmospheric stability length scale (similarity theory, Foken, 2006). T_c and T_s were verified by testing the estimated LE for a negative value, in which case temperatures are not correct, and the soil is assumed to have a dry surface. A new iteration cycle is needed, in which LE is set to zero for the soil component and H_s is re-calculated ignoring LE for the soil. A new T_s and T_c values are found and sensible heat flux components are again estimated, and canopy LE computed.

ET Extrapolation and Interpolation Methods

Evaporative Fraction Method (EF)

The EF extrapolation method is described below:

$$ET_{d\_EF} = 86{,}400\ EF\ (R_{nd} - G_d) / (\lambda_{LE}\ \rho_w) \quad (7)$$

$$EF = LE / (R_n - G)_i \quad (8)$$

$$R_{nd} = (1 - \alpha)\ R_{sd} - 110\ \tau_{sw} \quad (9)$$

where, ET_{d_EF} is daily ET (mm d^{-1}) obtained from extrapolating instantaneous (hourly) LE values to daily values using the EF method. The number 86,400 is the number of s d^{-1}, R_{nd} and G_d are average daily net radiation and soil heat flux respectively (in units of W m^{-2}), λ_{LE} is the latent heat of vaporization (M J kg^{-1}), equal to (2.501 – 0.00236 T_a), being T_a in º C units. ρ_w is water density (~ 1 Mg m^{-3}). G_d was ignored in Eq. 7 because it is a flux that is not commonly modeled (difficult to estimate) and because in most cases it tends to be zero, i.e. when the energy absorbed by the soil during the daytime is released during the nighttime causing $G_d \rightarrow 0$. Net radiation and soil heat flux with subscript "i," in Equation 8, indicates estimated "instantaneous" values.

R_{nd} expressed in Eq. 9 was proposed by De Bruin (1987); where α is surface albedo (dimensionless), R_{sd} is the average daily incoming (shortwave) solar radiation (W m^{-2}) and τ_{sw} is the shortwave atmospheric transmittance (dimensionless). In this study, R_{sd} was calculated by averaging mean hourly R_s values, measured at the ARS-Bushland weather station (Location marked with an “x” in Fig. 1) with a Pyranometer (LI-COR, Lincoln, Nebraska), for the entire day; while τ_{sw} was obtained using MODTRAN4.

Grass Reference ET Fraction Model

The second method, of ET_i extrapolation, used was the ET_oF or grass reference ET fraction method.

$$ET_{d\_EToF} = ET_oF \times ET_{od} \tag{10}$$

$$ET_oF = ET_i / ET_{oi} \tag{11}$$

$$ET_i = (3{,}600 \times LE) / (\lambda_{LE}\ \rho_w) \tag{12}$$

where, ET_{d_EToF} is daily ET (mm d^{-1}) extrapolated from instantaneous LE values using ET_oF. ET_{od} is daily grass reference ET, calculated by adding up the hourly grass reference ET (ET_{oi}, mm h^{-1}) over a 24 h period. ET_{oi} was calculated using the ARS-Bushland weather station hourly data and the ASCE-EWRI (2005) standardized Penman-Monteith method. ET_i is the TSM estimated instantaneous ET (mm h^{-1}).

Seasonal ET Method

The interpolation method used to infer on ET rates (cumulative) for a month or season was that utilized by Allen et al. (2002). In this model, ET_d, for a given day (in a given month) is expanded proportionally to the reference evapotranspiration of that month (cumulative ET). In our case, the reference crop ET was the grass reference ET_o. The underlying assumption is that ET changes in proportion to the change in the reference ET at the index weather site.

The first step was to determine the period represented by each image. In our case, the June 25 image represented the June month period, the July 10 image represented the period from July 1 to July 18, while the July 26 image represented the period from July 19 to July 31. The second step was to compute ET_o for the period represented by each image. Cumulative ET_{od}, for the period in consideration, was computed by adding up daily ET_{od} values. The third step was to compute the cumulative ET for each period as follows:

$$ET_{period} = ET_oF_{period} \sum_{i=1}^{n} ET_{od} \tag{13}$$

where, ET_oF_{period} is the representative ET_oF for the period, n is the number of days in the period. Units for ET_{period} will be “mm” when ET_{od} is in mm d^{-1}. Finally, the fifth step was to compute the seasonal ET by summing all the ET_{period} values for the length of the season considered.

Verification of the Two Source Model ET Estimation

Estimated ET values, both instantaneous and daily, were verified by comparison to ET derived from a soil-water mass balance using data from four large monolithic weighing lysimeters located at the USDA-ARS, CPRL.

The lysimeters (3 m long × 3 m wide × 2.4 m deep) were situated in the middle of 4.7-ha fields. In 2007, the lysimeter fields, northeast (NE, Fig. 1) was planted to forage sorghum (planted on May 30), the southeast (SE, Fig. 1) was planted to corn (planted on May 17) both for silage production, the northwest (NW, Fig. 1) was planted to grain sorghum in rows (planted on June 6), while the southwest (SW, Fig. 1) lysimeter field was planted to grain sorghum (planted on June 6) in clumps as part of a different research project. Furthermore, the NE and SE lysimeter fields were irrigated while the NW and SW lysimeter fields were managed under dryland conditions.

Each lysimeter field was equipped with one net radiometer [Q*7.1, Radiation and Energy Balance Systems (REBS), Bellevue, Washington] and one infra-red thermometer, (Exergen, Watertown, Massachusetts) for measuring net radiation and radiometric surface temperature, respectively.

Errors between estimated and observed ET values (instantaneous, daily and seasonal) were reported as mean bias errors (MBE) and root mean square errors (RMSE). Besides ET, predicted net radiation (instantaneous and daily) was verified with measured data and differences were reported as MBE and RMSE.

Results and Discussion

Net Radiation Estimation

Remote sensing based instantaneous net radiation estimates (R_n estimated, Fig. 3) compared well with observed (R_n observed, Fig. 3) values.

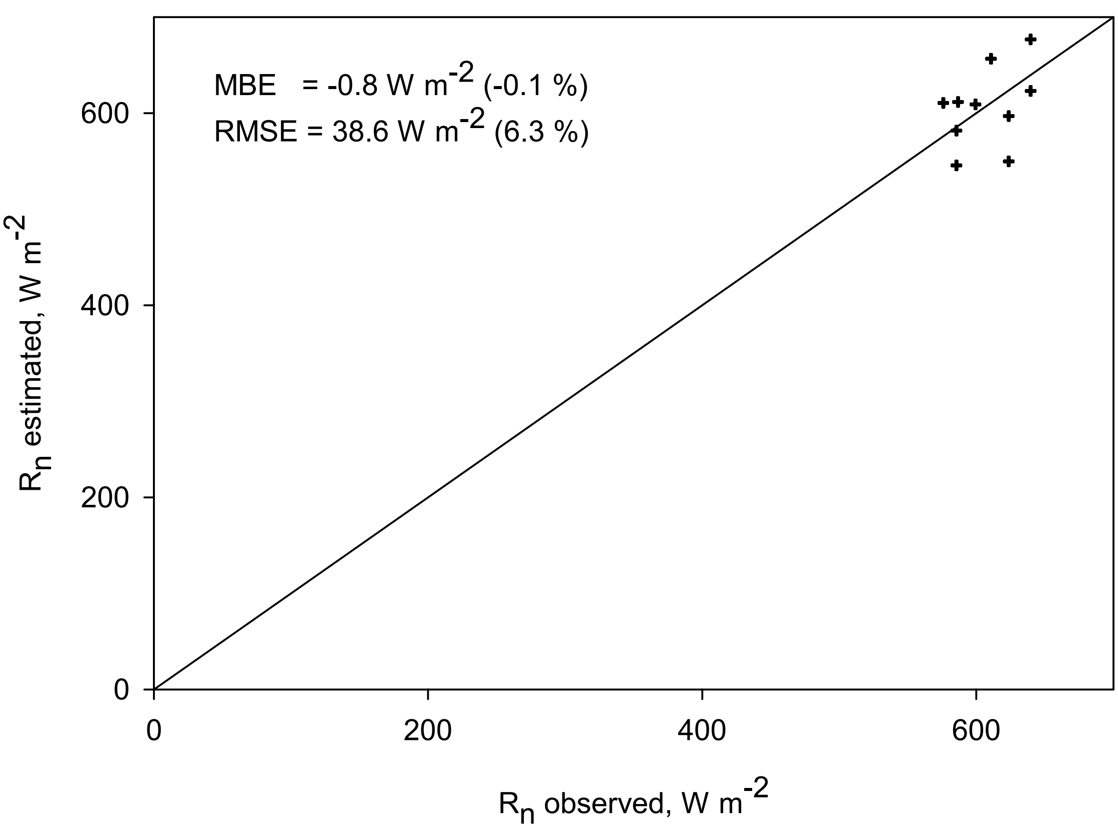

Figure 3. Estimated vs. observed instantaneous net radiation comparison.

Errors were normally distributed, i.e. almost proportionally on both sides of the 1:1 line, with a slight under estimation of 0.82 W m^{-2} (0.1%) and an average difference standard deviation of 38.61 W m^{-2} (or 6.3% error); which shows a very small error spread.

In the case of the daily net radiation, estimates (R_{nd} estimated, Fig. 4) very closely matched observed (R_{nd} observed, Fig. 4) values. Mean bias errors were -3.93 W m^{-2} (-2.2%) with an average difference standard deviation of just 4.0 W m^{-2} (only 2.3%) indicating that the model proposed by De Bruin (1987) performed well. It is worth mentioning that the daily solar radiation that goes into the model was calculated using hourly averages of incoming solar radiation measured with a Pyranometer, and the atmospheric transmittance for shortwave was calculated using the software MODTRAN4.

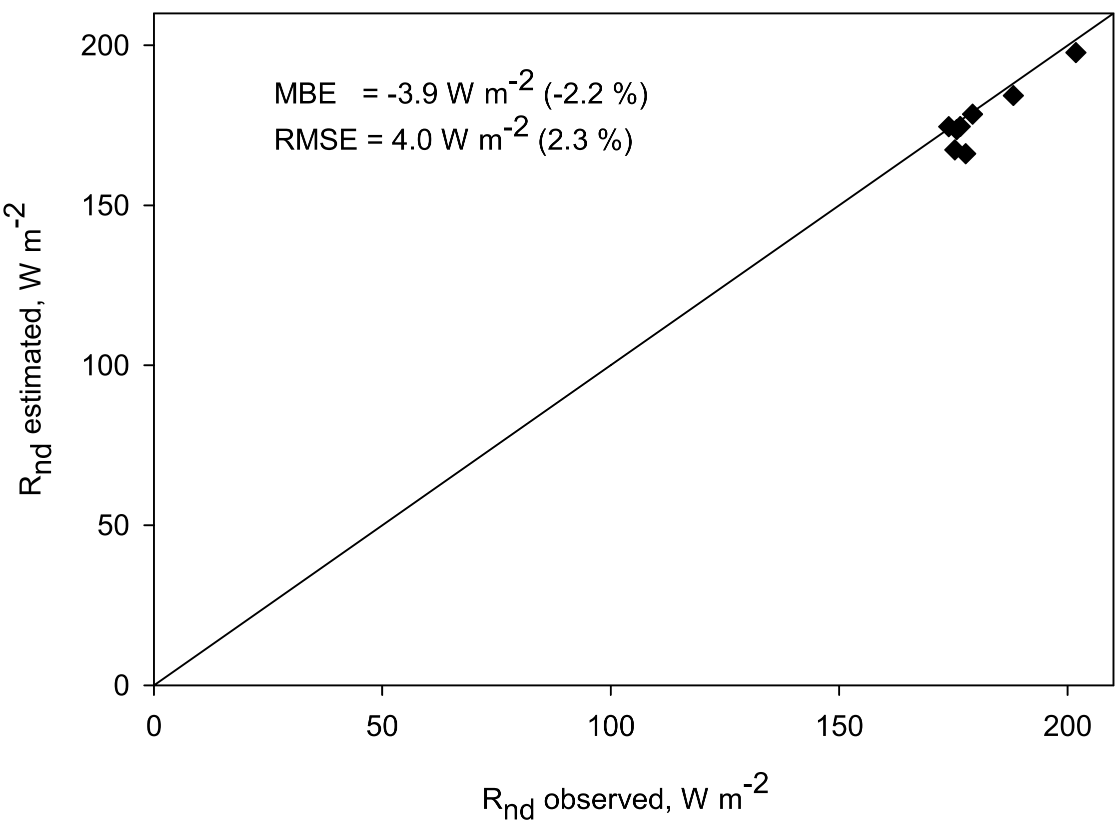

Figure 4. Estimated vs. observed daily net radiation comparison.

Hourly, Daily and Seasonal ET Estimation

For DOY 176, the TSM yielded hourly ET estimates for the NE and SE lysimeters fields that compared well with measured values, with a 6.82 and 7.46 absolute percent difference (APD) respectively; while for the NW and SW fields estimates resulted in large errors, 81.4 and 77.5 APD. These rather large errors, on the grain sorghum fields, most probably occurred due to the inability of the TSM to account for heterogeneous surfaces depicting very low biomass (LAI ≈

0.5 m^2 m^{-2}) and considerable bare soil presence (soil fraction cover (F_s) of 0.84), as in DOY 176 (see Figure 1 (a)). Under these circumstances, surface friction velocity (u*) and surface aerodynamic resistance may not be well estimated. These terms depend on the zero plane displacement (d, m), the roughness length for momentum transfer (Z_{om}, m), and the roughness length for heat transfer (Z_{oh}, m); which were calculated according to Brutsaert (1982) as a function of crop height (h_c, m). Brutsaert (1982) empirically developed the relationships, between h_c and the parameters mentioned above, under more homogeneous surfaces conditions. Therefore, d, Z_{om}, and Z_{oh} may have introduced errors into u* and r_{ah}. To correct for probable errors in u* and r_{ah}, which affect H_s, we neglected r_{ah} in Equation 4 and r_s was calculated assuming U_s equal to the wind speed at the canopy level (U_c).

After processing the adjustments described above, errors in the estimation of ET_i for the NW and SW fields were reduced to 15.0 and 6.3 % respectively (DOY 176). On the other hand, for DOY 191, changing how H_s was calculated did not improve ET_i results, LAI values were above 0.7 m^2 m^{-2}, approaching 1.0 for both NW and SW fields, and F_s values were smaller than 0.70 for all fields. ET_i estimated without modifications to H_s resulted in a slight under estimation for lysimeter fields NW and SW, with a -7.83 and -5.16 APD respectively. Contrastingly, there was an over estimation for the NE and SE fields, with an APD of 27.46 and 24.94 respectively (DOY 191). For these fields, LAI was 2.1 and 4.6 m^2 m^{-2} respectively. The main reason for ET over estimation on the NE and SE fields may have been an irrigation event just half an hour before the remote sensing system overpass. An irrigation event occurred from about 10:00 am CST to about 11:00 am CST at the NE and SE lysimeters sites. Fig. 1 (b) shows the position of the Linear Move irrigation system (oriented North-South) traveling easterly. Field records indicated that during DOY 191, 18 mm (0.72 in) of water were applied on the NE and SE fields. Also in Fig. 1 (b), west of the Linear Move system, surface reflectance values were lower than in the east side due to wet canopy/soil radiation absorption in the visible electromagnetic spectrum. Lower reflectance values may have affected surface (composite) albedo, soil albedo, vegetation indices, as well as the calculation of d, Z_{om}, and Z_{oh} on the wet/cooler pixels.

For DOY 207, ET_i was also over estimated for the NE and SE lysimeters fields, with 18.75 and 17.96 APD respectively. ET_i for the NW and SW fields was slightly under estimated, -7.83 and -8.06 APD respectively. The over prediction may have been caused by errors in the estimation of the fraction of LAI that is green, the clumping factor (Ω), the vegetation fraction, soil heat flux, and/or the soil resistance to heat flux term when LAI was around 5.0 m^2 m^{-2} (NE and SE fields, DOY 207).

ET_i estimation errors for all three DOYs, including changes in H_s estimation for NW and SW lysimeters sites, resulted in a MBE of 0.05 mm h^{-1} (or 8.15% error), and a RMSE of 0.10 mm h^{-1} (or 14.39%). Overall, this is a low error as depicted in Fig. 5; where predicted values closely matched with observed low ET rates (closer to the 1:1 line). Most of the errors were contributed by the large ET over estimation errors associated with the NE and SE lysimeters fields on DOY 191 and 207 (circled squares, Fig. 5).

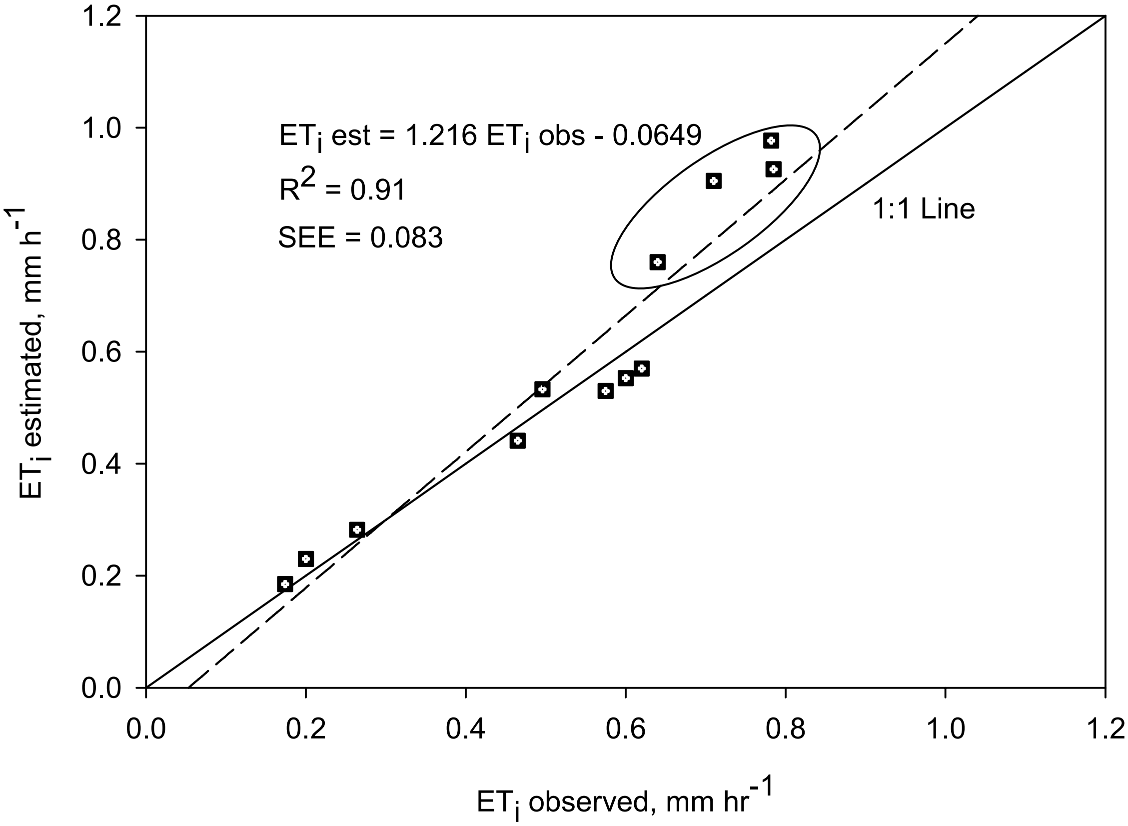

Figure 5. Comparison of estimated vs. observed hourly (instantaneous) evapotranspiration (ET_i).

In the case of daily ET prediction, the evaporative fraction (EF) extrapolation method under estimated true average ET_d by -0.8±0.8 mm d^{-1} (MBE±RMSE), or in percent -8.7±17.4% error. Better ET_d estimates resulted with the grass reference ET fraction (ET_oF), errors in estimating true ET_d were 0.6±0.8 mm d^{-1}, or 12.4±14.9%. In addition, Fig. 6 shows a closer agreement between estimated and observed ET_d values for the ET_oF extrapolation method (better agreement with the 1:1 line). The irrigation event of DOY 191 was the main cause of the over estimation (as much as 31.4 % for NE lysimeter and 21.5 % for the SE lysimeters). Between 6:00 to 10:00 a.m. CST the NE and SE fields had not been irrigated consequently had ET rates lower than the rates after 10:00 a.m. when irrigation occurred. Therefore, the TSM with remote sensing inputs at 11:30 a.m. over estimated ET_d because the system used lower surface temperatures which were extrapolated for the entire day, in the estimation of daily ET, when in reality there was a period during the day that the surface temperatures were higher and ET was lower. This short period of lower ET rates was not accounted for in the TSM algorithm that used the airborne remotely sensed surface albedo and temperature.

Nevertheless, if we correct ET_i for the period of the day that the NE and SE fields were not irrigated, and obtain lower ET_d values, we will see that the ET_oF method out performs the EF method because the EF would have even higher under prediction values, at the irrigated lysimeters fields, thus increasing its overall ET_d estimation error.

Similar results were obtained by Chávez et al. (2007) when the TSM was applied to a Landsat 5 TM image. In that study, the TSM in general under predicted ET_d by -0.8±0.8 mm d^{-1}, or in percent by -9.2±9.0%; although larger errors were evident on the lysimeters fields with LAI greater than 3.0 m^2 m^{-2}, The extrapolation method used in the study was the EF; which, then seems to tend to under predict ET_d for the advective condition of the THP.

As an example that advection occurred, at the time of the aircraft overpass for DOY 191, the sensible heat flux was -37.4 W m^{-2} and for DOY 207 it was -30.4 W m^{-2} at the SE forage corn irrigated lysimeters field. Air temperature was larger than the canopy and the aerodynamic temperature, therefore indicating that extra heat was advected to the irrigated surface.

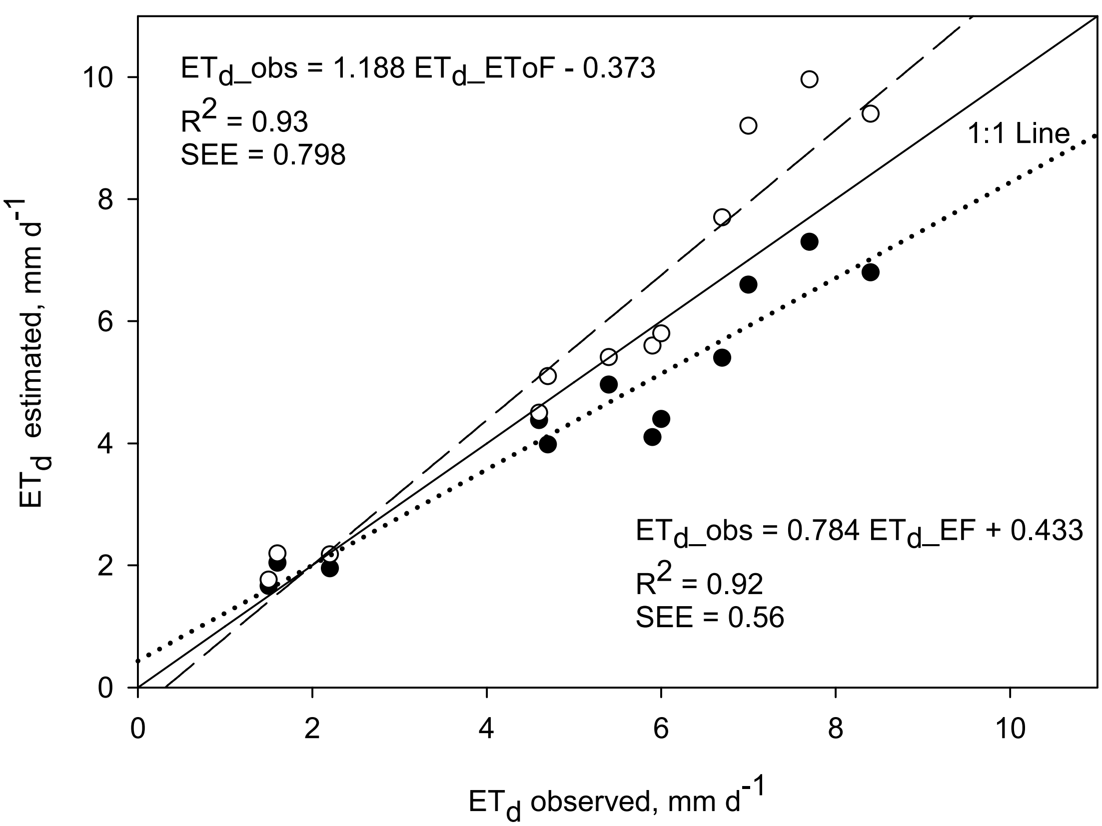

Figure 6. Comparison of estimated vs. observed daily evapotranspiration (ET_d).

Estimating monthly ET using ET_oF as an interpolation factor resulted in an ET under estimation of 5.5±16.7 mm (10.8±19.6 %) for the month of June, and 1.1±46.9 mm (0.9±27.3 %) for the month of July. For the short season comprised by the months of June and July together (June+July) the overall error was relatively small, -8.9±30.4 mm or -3.6±12.5 %. Cumulative ET values for June, July, and June+July, including error bars, can be seen in Figure 7 below.

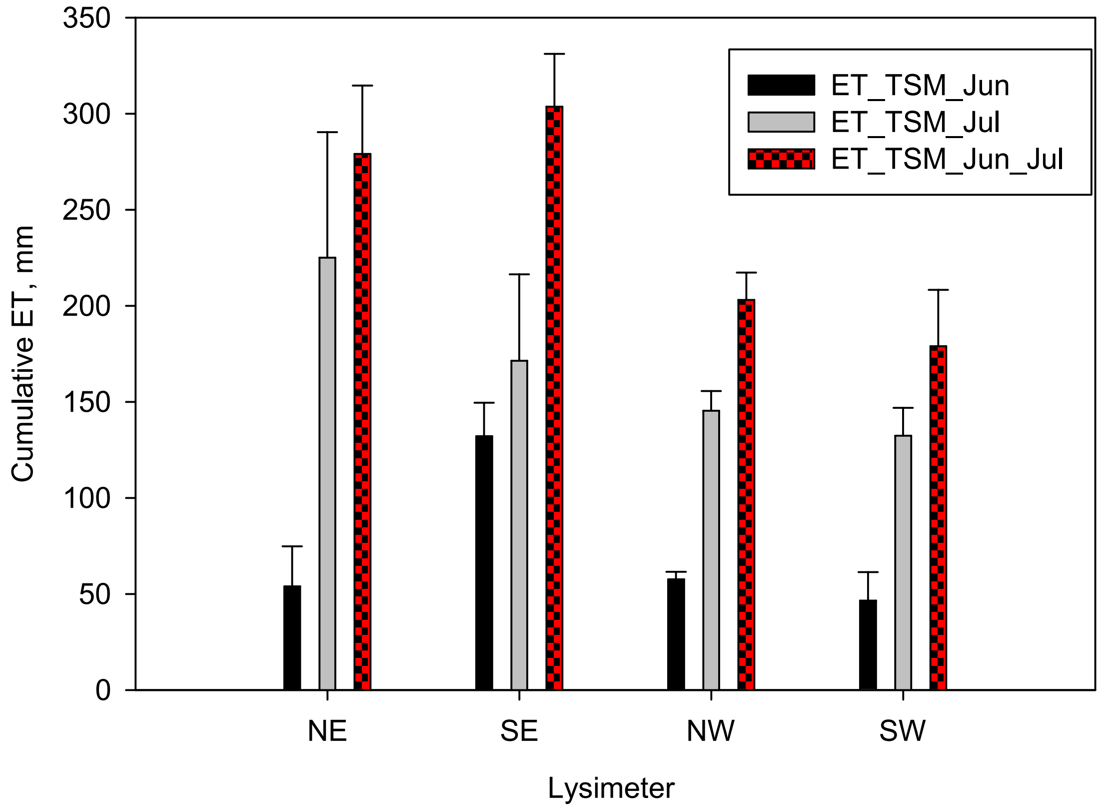

Figure 7. Comparison of estimated vs. observed cumulative evapotranspiration.

In the vertical bars of Fig. 7, larger errors can be seen for the July cumulative ET values (column, ET_TSM_Jul); which were introduced by the over estimation of ET_i during DOY 191. Considering the impact that ET_oF obtained in a given day can have on the generalization of ET_oF for a given period, and the posteriori estimation of cumulative ET, it is recognized that there is a need to investigate mechanisms to compensate for situations where agricultural fields have been irrigated during a portion of the day and during the remote sensing system overpass. Otherwise, ET_oF apparently works well in estimating seasonal (cumulative) ET values.

Conclusion

In this study, a two source energy balance model (TSM) was applied on three high resolution airborne remote sensing multispectral imagery, during the 2007 cropping season, to estimate instantaneous evapotranspiration values in the advective semi-arid region of the Texas High Plains. In addition, two mechanisms to extrapolate instantaneous ET predictions to daily values and a method to estimate seasonal ET were tested.

Instantaneous ET was predicted with an overall RMSE of 0.10 mm h^{-1} (14.39%). Most of the over prediction errors were contributed by ET values from forage corn (SE) and sorghum (NE) fields that were irrigated just prior to the remote sensing system overpass on DOY 191. Other over prediction errors occurred on DOY 207 on the NE and SE lysimeters fields. We speculate that the fraction of LAI that is green, the clumping factor (Ω), the vegetation fraction, soil heat flux, and/or the soil resistance to heat flux term, when LAI is around 5.0 m^2 m^{-2}, may have caused the ET over prediction. These terms need to be further investigated. In addition, the aerodynamic resistance term in the estimation of the soil sensible heat flux, for DOY 176, was neglected because Brutsaert's (1982) fractions to estimate zero plane displacement, surface roughness length for momentum and heat transfer did not apply under the biomass and surface heterogeneity conditions of the dryland grain sorghum planted in the NW and SW lysimeters fields.

TSM instantaneous ET extrapolated to daily values using the grass reference ET fraction method performed better than the evaporative fraction method. Their prediction errors were, 0.6±0.8 mm d^{-1} (12.4±14.9%) and -0.8±0.8 mm d^{-1} (-8.7±17.4%) respectively. Grass reference ET fraction based daily ET values closely matched with the lysimeter derived ET values.

Cumulative or seasonal ET was well predicted using the remotely sensed grass reference ET fraction as a monthly (or shorter period) interpolation index. Estimation errors for the short season comprising the months of June and July were -8.9±30.4 mm (-3.6±12.5%). It appears that the key to a successful monthly/seasonal ET estimation is the proper identification of a grass reference ET fraction that is representative of the period (days, week, or month).

Acknowledgements

This study was possible thanks to funding provided through the Ogallala Aquifer Program. Our sincere appreciation to the following individuals who provided assistance: Donald A. Dusek, Kim Bush, Osama Akasheh, Sivarajan Saravanan, and Saleh Taghvaeian.

References

Allen, R.G., M. Tasumi, and R. Trezza. 2007. Satellite-based energy balance for mapping evapotranspiration with internalized calibration (METRIC)-model. *ASCE J. of Irrig. and Drain. Eng.* 133(4): 380-394.

Allen, R.G., M. Tasumi, and R. Trezza. 2002. *METRIC™: mapping evapotranspiration at high resolution – application manual for Landsat satellite imagery*. University of Idaho, Moscow, ID.

ASCE-EWRI. 2005. The ASCE standardized reference evapotranspiration equation. Report by the American Society of Civil Engineers (ASCE) Task Committee on Standardization of Reference Evapotranspiration. Allen, R.G., I.A. Walter, R.L. Elliot, T.A. Howell, D. Itenfisu, M.E. Jensen, and R.L. Snyder (eds.), ASCE, 0-7844-0805-X, 204 pp., Reston, VA.

Bastiaanssen, W.G.M., M. Menenti, R.A. Feddes, and A.A. Holtslang. 1998. A remote sensing surface energy balance algorithm for land (SEBAL): 1. Formulation. *J. of Hydrol.* 212-213:198-212.

Berk, A., G.P. Anderson, P.K. Acharya, M.L. Hoke, J.H. Chetwynd, L.S. Bernstein, E.P. Shettle, M.W. Matthew, and S.M. Adler-Golden. 2003. MODTRAN4 version 3 revision 1 user's manual. Air Force Research Laboratory, Space Vehicle Directorate, Air Force Materiel Command, Hanscom AFB, MA 01731-300, Hanscom.

Brutsaert, W., M. Sugita. 1992. Application of self-preservation in the diurnal evolution of the surface energy budget to determine daily evaporation. *J. of Geophys. Res.* 97:18,377-18,382.

Brutsaert, W.H. 1982. *Evaporation into the atmosphere*. Boston, MA: D. Reidel.

Chávez, J.L., P.H. Gowda, T.A. Howell, and K.S. Copeland. 2007. Evaluating three evapotranspiration mapping algorithms with lysimetric data in the semi-arid Texas High

Plains. In *Proc. 28th Annual International Irrigation Show*. 268-283, Irrigation Association 2007 CDROM.

Chávez, J.L., C.M.U. Neale, L.E. Hipps, J.H. Prueger, and W.P. Kustas. 2005. Comparing aircraft-based remotely sensed energy balance fluxes with eddy covariance tower data using heat flux source area functions. *J. of Hydromet.* 6(6):923-940.

De Bruin, H.A.R. 1987. From Penman to Makkink. In *Proc. and information of the TNO Committee on Hydrological Research*. Hooghart, J.C. ed., 39: 5-31 Gravenhage, The Netherlands.

Colaizzi, P.D., S.R. Evett, and J.A. Tolk. 2006. Comparison of five models to scale daily evapotranspiration from one-time-of-day measurements. *Trans. of ASABE* 49(5) 1409-1417.

Foken, T. 2006. 50 Years of the Monin-Obukhov similarity theory. *Boundary-Layer Meteorol*. 119(3): 431-447.

Gowda, P.H., J.L. Chavez, P.D. Colaizzi, S.R. Evett, T.A. Howell, and J.A. Tolk. 2008. ET mapping for agricultural water management: Present status and challenges. *Irrig. Sci.* 26(3):223-237, DOI 10.1007/s00271-007-0088-6.

Gowda, P.H., J.L. Chávez, P.D. Colaizzi, S.R. Evett, T.A. Howell, and J.A. Tolk. 2007. Remote sensing based energy balance algorithms for mapping ET: Current status and future challenges. *Trans. ASABE* 50(5): 1639-1644.

Jackson, R.D., T.R. Clarke, and M.S. Moran. 1992. Bidirectional calibration results of 11 Spectralon and 16 BaSO4 reference reflectance panels. *Remote Sens. of Env*. 40: 231-239.

Kustas, W.P., and J.M. Norman. 2000. A two-source energy balance approach using directional radiometric temperature observations for sparse canopy covered surfaces. *Agron. J*. 92:847-854.

Menenti, M., and B.J. Choudhury. 1993. Parameterization of land surface evapotranspiration using a location dependent potential evapotranspiration and surface temperature range. In *Proc. Exchange Processes at the Land Surface for a Range of Space and Time Scales*. 561-568, Bolle HJ et al. (eds), IAHS Publ. 212.

Neale, C.M.U., and B. Crowther. 1994. An airborne multispectral video/radiometer remote sensing system: development and calibration. *Remote Sens. of Env.* 49(3): 187-194.

Norman, J.M., W.P. Kustas, and K.S. Humes. 1995. A two-source approach for estimating soil and vegetation energy fluxes form observations of directional radiometric surface temperature. *Ag. and Forest Meteorol.* 77:263-293.

Priestly, C.H.B., and R.J. Taylor. 1972. On the assessment of surface heat flux and evaporation using large-scale parameters. *Mon. Weather Rev*. 100: 81-92.

Su, Z. 2002. The surface energy balance system (SEBS) for estimation of turbulent heat fluxes. *Hydrol. and Earth Syst. Sci.* 6:85-99.

Sundararaman, S., and C.M.U. Neale. 1997. Geometric calibration of the USU videography system. In *Proc. 16th Biennial Workshop in Videography and Color Photography for Resource Assessment*. American Society of Photogrammetry and Remote Sensing, Bethesda, MD.

Trezza, R. 2002. Evapotranspiration using a satellite-based surface energy balance with standardized ground control. PhD dissertation, Logan, Utah: Utah State University, Biological and Irrigation Engineering Department.